Enzyme kinetics, self-organized molecular machines, and parametric resonance

Manfred Schienbein and Hans Gruler
Complex Fluids Group, Biophysics Department, University of Ulm, D89081 Ulm, Germany
and Centre d'Écologie Cellulaire, Hôpital de la Salpétrière, 47 Boulevard de l'Hôpital, F75651 Paris Cedex 13, France
(Received 11 July 1997)

Different models of enzymatic reactions are discussed and compared with experiments (a cytochrome P-450-dependent mono-oxygenase system). The following results are obtained. (i) Every chemical step in the reaction cycle contains approximately 5–7 substeps (approximately 40–60 steps in the cycle). (ii) In the case of too many substeps, the reaction cycle can be approximated by a continuous model. A Fokker-Planck equation is derived with drift and diffusion. The drift coefficient is determined by the measured cycle time (1.54 s) and the diffusion term by the measured memory time (2.8 times the cycle time). (iii) The enzymatic reaction can be influenced by periodic external signals. The action spectrum is described by a stochastic and parametric resonance. [S1063-651X(97)04312-2]

PACS number(s): 87.10.+e, 87.15.Rn, 87.50.−a

INTRODUCTION

Many scientists are fascinated by the ability of single macromolecules like enzymatic proteins to act like a whole chemical production plant. A physical description of such small-sized production factories is the topic of this paper.

A well-made machine or robot in the technical world is constructed by using mainly deterministic processes, e.g., the information flux diagram of a computer. One might expect that small-sized chemical production factories (enzymes) can be understood in the framework of deterministic processes, since the sequence of chemical reactions can be ordered in a reaction cycle [1]. But one has to remember that every macroscopic system is subject to fluctuations and noise and, thus, the physical state of a system is determined by the interplay of deterministic and stochastic processes [2]. The direction in which a system will proceed is mainly given by the deterministic processes and the speed of state changes by the stochastic processes. It will be shown how the mean deterministic and stochastic process of an enzymatic reaction can be determined. A few examples where stochastic and deterministic processes are involved are as follows:

(1) Irregular movement of small colloidal particles is caused by the impacts of the molecules of the liquid. An applied force is the cause for the mean drift of the colloidal particles [3,4].

(2) Fluctuations in emission-limited flow in thermionic diodes is carried by single and independent emitted electrons. An applied electric field is the cause for the mean drift of the electrons [5–7].

(3) Random migration of cells is caused by stochastic processes in the cellular signal transduction chain. An applied extracellular guiding signal is the cause for the mean drift of the cells [8].

The modern analysis of stochastic processes was introduced by Kramers [9] and Brinkman [10]. They treated the escape from a potential well as a problem of Brownian motion in a nonuniform force field. Thus even complex nonequilibrium systems can often be reduced to equilibrium systems with only a few degrees of freedom by the elimination of dynamically nonrelevant variables [11].

This approach consists of assuming that the system can be described by a set of random variables which change either discretely or continuously in their state space. In the former case of discrete changes, the state of variables is described by a set of discrete states. The system is characterized by a discrete probability distribution function, which is the probability of the variables being in a certain state at a given time. The system is assigned a set of transition probabilities per unit time for the process to go from one state to another. The form of these transition probabilities depends on the process, and reflects the nature of the interactions in the complex system. The equation describing the evolution in time of the probability distribution of the system's variables is the so-called master equation, which is a set of differential equations, first order in time. To simplify the problem only transitions between nearest-neighboring states are considered. The random process describing such systems is called a univariate birth and death process. When the random variables defining the system change continuously, the system is characterized by a probability density function that satisfies a second-order partial differential equation, the so called Fokker-Planck equation. The enzyme kinetics will be discussed in the framework of master equations (discrete states) as well as of the Fokker-Planck equation (continuous states). The motion within an enzyme is enormous since every atom performs a movement. But this huge number of modes is reduced to two relevant ones: (i) the drift mode, and (ii) the diffusion mode.

Next, details of an enzymatic reaction will be discussed. But we keep the discussion on the reaction cycle very general, so that it can hold for any type. We will demonstrate the principle with a very complex enzyme—the cytochrome P-450 mono-oxygenase system [12]. The protein complex, consisting of the enzyme P-450 and the NADPH-cytochrome P-450 reductase, can be reconstituted in vitro [13,14]. The protein complex transforms e.g., the substrate, 7-ethoxycoumarin, into the product, 7-hydroxycoumarin, which can be detected spectroscopically. The enzyme P-450 is the Rosetta stone among the heme-containing mono-oxygenases [12]. This enzyme plays an important role in the oxidative metabolism of lipophilic substrates in eukaryotic

and prokaryotic species [15,16]. The basic biochemical reactions of this enzyme are known, but the physical description of such small-sized working chemical production plants are not well established.

At the start of this century, Michaelis and Menten approximated the action of an enzyme by the following reaction scheme [1]:

$$S+E \overset{K_S}{\rightleftharpoons} ES \overset{k_E}{\rightarrow} EP \overset{K_P}{\rightleftharpoons} E+P.$$

First, the substrate molecule S binds reversible to the enzyme E (equilibrium binding coefficient K_S); second, the enzyme-substrate complex ES is irreversibly transformed into the enzyme-product complex EP (transduction coefficient k_E); third, the product molecule P binds reversibly to the enzyme (equilibrium binding coefficient K_P); fourth, the total amount of enzyme is conserved ($E+\mathrm{ES}+\mathrm{EP}=E_0=\mathrm{const}$). The production rate dP/dt or the enzyme activity $(dP/dt)E_0^{-1}$ is

$$\frac{dP}{dt}\frac{1}{E_0}=k_E\frac{\dfrac{S}{K_S}}{1+\dfrac{S}{K_S}+\dfrac{P}{K_P}}. \tag{1}$$

The maximum enzyme activity obtained for high substrate concentrations ($S \gg K_S$) and low product concentrations ($P \ll K_P$) is determined by the transduction coefficient k_E or the duration τ ($=1/k_E$) of one cycle. In the case of the reconstituted P-450 complex, the maximum activity is obtained by extrapolating the enzyme activity measured at low product concentrations to infinite high reductase and substrate concentrations. The measured transduction coefficient and cycle time are of 0.65 s^{-1} and 1.54 s, respectively [14]. (The cytochrome P-450_{2B1} form is isolated from phenobarbital treated rats.)

One possible way to obtain the value of the transduction coefficient k_E is the determination of the maximum enzyme activity, but this method is very time and material consuming. Another method is based on synchronized enzymes [17,18]: Usually one has incoherently working enzymes, where each enzyme works independently of the other ones. The phase relation between the cycles of different enzymes is random and, thus, the product concentration in the test tube increases linearly in time (see the dashed line in Fig. 1). But, in the case of synchronized enzymes, the cycles of the enzymes work with a fixed phase relation (equal to coherently working enzymes) and, thus, the expected product concentration in the test tube increases by a step when the product molecules are released (see the solid line in Fig. 1). The cycle time can be determined by measuring the time difference between two consecutive steps in the product concentration. The memory time τ_M describes the randomization process in the phase relation of different working enzymes. It can be determined by measuring the extrapolated product release at consecutive cycle times as will be shown below. A few words about synchronization mechanisms:

(i) One method is based on an autocatalytic reaction, where the first stage of the cycle is externally regulated [19].

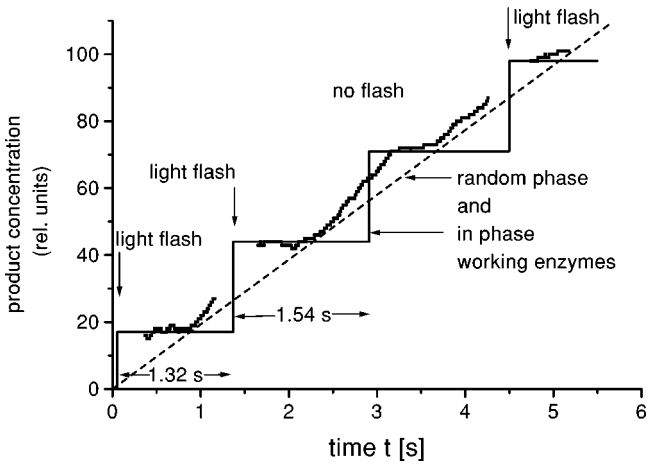

FIG. 1. The spectroscopically measured product concentration (7-hydroxycoumarin) as a function of time at 30 °C (reconstituted system, see Ref. [14]; fluorescence measurement, see Refs. [17] and [18]). The excitation wavelength was 365 ± 8 nm. The detected emission wavelength was 460 ± 10.5 nm. The second light source was adjusted to the action spectrum of the catalytic reaction (wavelength: 420 ± 10 nm; irradiation time: 0.1 s; repetition time: 1.32 s; energy: 0.27 J/nM P-450). The dots are the actual measurement. The straight dashed line is the prediction for in random phase working enzymes and the solid line (step function) for in phase working (synchronized) enzymes.

Coherently working enzymes are obtained if a product-activated enzymatic reaction is assumed and the enzyme concentration is high enough.

(ii) Another method, which is actually used, is based on external applied signal. An enzymatic reaction can be enslaved by an external periodic signal if (a) there exists an interaction between the external signal and at least one state of the enzymatic reaction, (b) the repetition time of the external signal is comparable with the cycle time of the enzyme, (c) the memory time involved in the enzymatic reaction is large compared with the cycle time, and (d) stochastic processes are involved in the enzymatic reaction.

The application of periodic light pulses is one technique of synchronizing enzymatic reactions. The reaction rates in the catalytic cycle can be altered if one of the active groups of the enzyme complex absorbs light. The enzyme cycles work partially in phase [17,18] if the repetition time of the light flashes are slightly smaller than the catalytic cycle time of the free running enzyme (e.g., a 1.54-s cycle time and maximum synchronization at a repetition time of 1.32 s). A typical experimental result of the reconstituted P-450 system is shown in Fig. 1. The characteristic cycle time of the free running enzyme can be determined from the sudden increase in the product concentration after a synchronization pulse.

In summary, the transduction coefficient k_E ($=\tau^{-1}$) describes the deterministic processes of an enzymatic reaction as a whole. The cycle time τ can be obtained from (i) the maximum enzyme activity of nonsynchronized enzymes, and (ii) from sudden changes of product concentration of synchronized enzymes.

Next, the enzymatic reaction will be described by using the distinct chemical states of the reaction cycle.

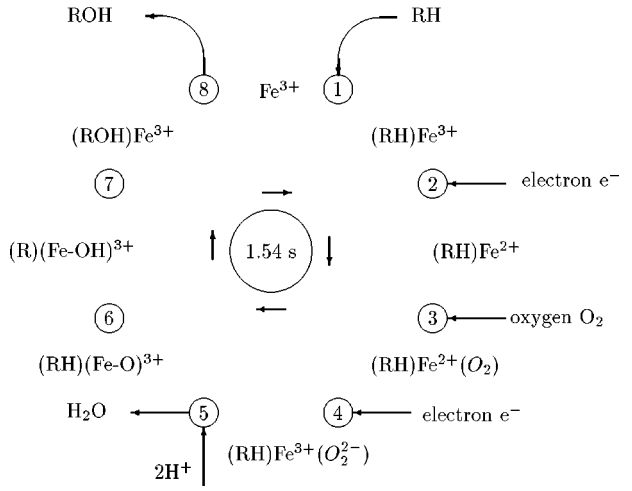

FIG. 2. A schematic representation of the reaction cycle of the mono-oxygenase system is shown: Step 1, the substrate molecule S (here RH) binds to the active group (Fe) of the enzyme. Step 2, the coenzyme delivers an electron and reduces the iron to Fe^{2+}. Step 3, an oxygen molecule in the aqueous solution binds to the active group. Step 4, the coenzyme delivers a second electron to the active group. Step 5, two protons of the aqueous solution bind to the active group, and a water molecule is released from the enzyme. Step 6, a specific hydrogen bond at the substrate molecule is opened and the hydrogen is transferred to the active group. Step 7, a hydroxyl group is brought from the active group to the substrate molecule. Step 8, the product molecule P (here: ROH) is released from the active group of the enzymes.

MODEL OF THE CLASSICAL ENZYME REACTION

An enzymatic reaction consists usually of several distinct chemical reactions. The catalytic cycle of P-450 contains, e.g., eight states (Fig. 2, Ref. [20]): The cycle starts when a substrate molecule like 7–ethoxycoumarin combines with the Fe^{3+} of the enzyme (step 1), which is then reduced by an electron originating from NADPH (energy source) to the Fe^{2+} form (step 2). [NADPH is the reduced form of NADP (nicotinamide adenine dinucleotide phosphate).] Then, the enzyme is oxygenated (step 3) and a second electron from NADPH converts the bound oxygen into the O_2^- radical (step 4). An internal oxidoreduction ensures, with the formation of the hydroxylated substrate and H_2O (steps 5–7). In the last state, the product molecule (e.g., 7-hydroxycoumarin) is released (step 8) after one characteristic cycle time τ. The enzyme is again ready to bind a new substrate molecule (step 1).

A set of reaction equations characterizes such an enzymatic reaction. The rate equation for the mth state is (Fig. 3)

$$\frac{dp_m}{dt} = -(f_m + b_m)p_m + f_{m-1}p_{m-1} + b_{m+1}p_{m+1}. \quad (2)$$

p_m is the probability to find an enzyme in the state m. The first term on the right side of this equation describes the efflux of the probability to the states $m+1$ (forward probability f_m) and $m-1$ (backward probability b_m), respectively. The second and third terms describe the influx from the state $m-1$ and $m+1$, respectively.

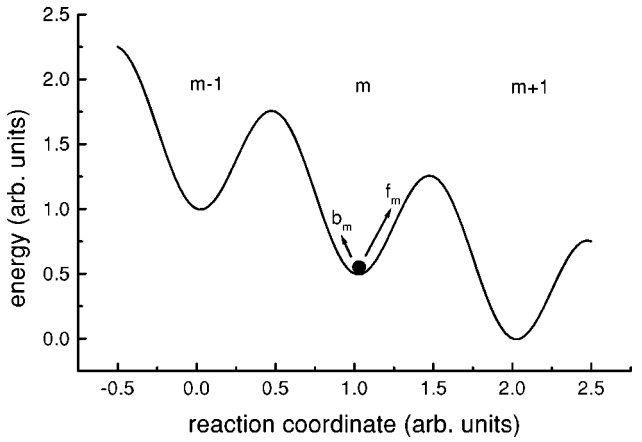

FIG. 3. A schematic representation of the mth step in the reaction cycle.

The M differential equations for an M-step catalytic cycle can be solved numerically for known coefficients f_m and b_m. For simplicity it is assumed that all steps in the cycle are similar. One might of course envisage more general scenarios, where not all reaction states are equally likely. We believe, however, that our model reduces arbitrariness to a bare minimum, still retaining sufficient generality to describe a set of reasonable enzyme reaction processes. The following results are calculated.

(1) The mean cycle time as well as the width of the cycle time distribution are a function of the transition probabilities. The cycle time distribution is a sharp peak if the forward reaction is much faster than the backward reaction ($f_m \gg b_m$), and the cycle time distribution is a very broad peak if the forward reaction is comparable with the backward reaction ($f_m \geqslant b_m$). Typical distributions are shown in Fig. 4.

(2) The product concentration as a function of time is calculated when all enzymes bind simultaneously a substrate molecule S at time zero. The product molecule P is released with a certain probability accordingly the calculated cycle time distribution. Thus the product concentration $P(t)$ for small times reflects the integrated cycle time distribution. The calculated product concentration increases linearly for long times, since the cycles have lost their phase relation [see Fig. 5(a)].

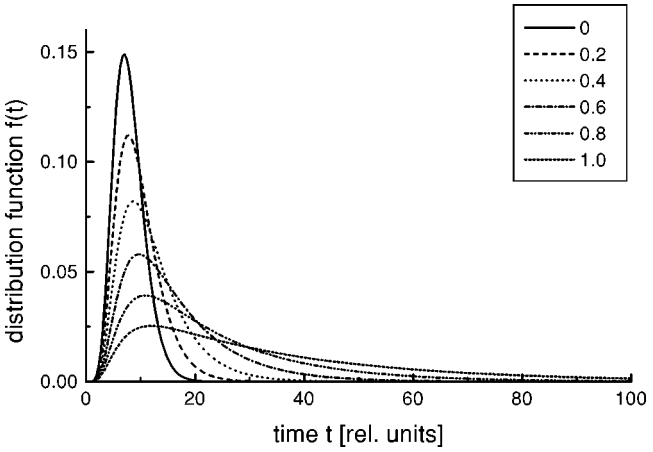

FIG. 4. The calculated reaction cycle distribution. The total number of steps is kept constant ($N=8$). The forward reaction is kept constant. But the ratio b_n to f_n is altered from 0 to 1.00.

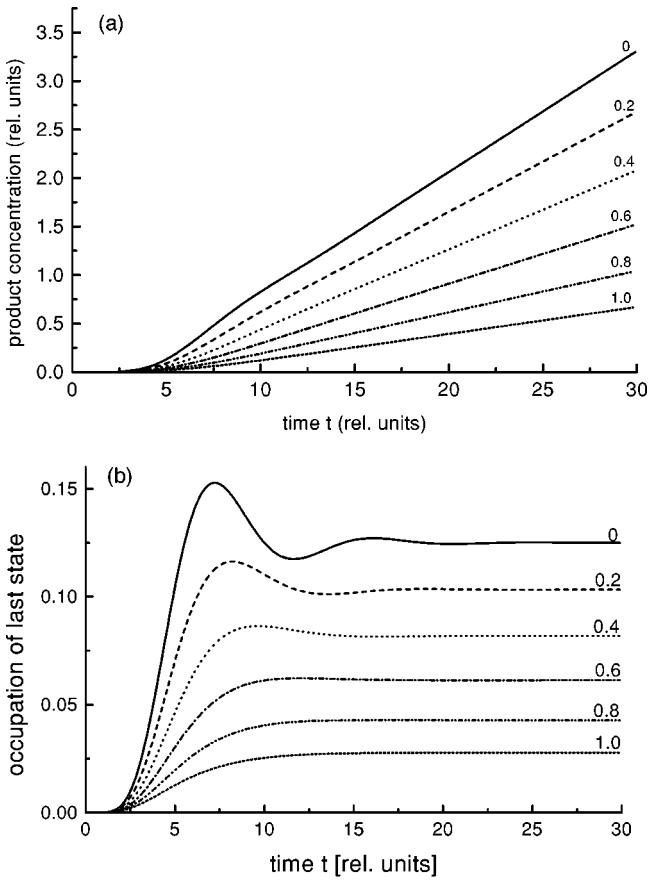

FIG. 5. (a) The calculated product concentration as a function of time. (b) The occupation of the last state in the reaction cycle. The reaction started at $t=0$. The total number of steps is kept constant (M=8). The forward reaction is kept constant. But the ratio b_n to f_n is altered from 0 to 1.00.

(3) The occupation of the last state P_8 in the reaction cycle is calculated [Fig. 5(b)]. The calculated curves show features of a damped oscillator. One important result is that the memory time of the enzymatic reaction, τ_M, is short compared with the cycle time τ. The normalized memory time τ_M/τ is ≈ 0.42 even in case of no back reaction ($b=0$). The normalized memory time decreases further in case of a finite back reaction coefficients.

The memory time of an enzymatic reaction can be experimentally determined in the following way [18]: First, the enzymes in a test tube are synchronized by periodically applied synchronization pulses (light flashes). Second, the extrapolated step height in the product concentration is measured at multiples of the cycle time, $t=\tau, 2\tau, 3\tau, \ldots$ after the last synchronization pulse (flash) (see Fig. 1 in Ref. [18]). A typical experimental result is given in Fig. 6. The measured normalized memory-time, τ_M/τ, of the reconstituted P-450 system is large [$\approx(2.8\pm 0.5)$], but the calculated one, based on eight states, is small (≈ 0.42). This discrepancy is a hint that the enzymatic model used has to be modified.

(4) The synchronization of the enzymatic reaction by a periodic external signal is predicted. The product concentration as a function of time can be calculated if at least one rate coefficient can be altered by an externally applied signal. The following results are obtained (Fig. 7): (i) The enzymatic reaction can be enslaved by an external signal. (ii) The

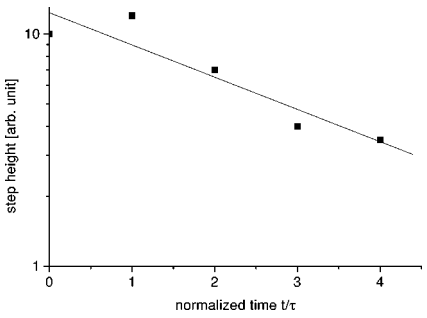

FIG. 6. The (extrapolated) step height is determined from the temporal function of the product concentration. The sudden increase in the product concentration is measured at multiples of the characteristic time τ.

enzymes show only medium percentages of synchronization ($\approx 40\%$). (iii) There are practically no changes in the percentage of synchronization if the repetition time of the synchronization pulses is varied.

These predictions are in contrast to the experimental results [18]: (i) The reconstituted enzyme complex can be synchronized up to high percentages (over 80%). (ii) A well-structured synchronization curve is measured (see Fig. 2 in Ref. [18]). Two peaks with high synchronization are observed. The repetition time for the first peak is between 1.25 and 1.5 s, and the repetition time for the center of the second peak is close to twice the cycle time. The previously published data [18] are confirmed by recent experiments [21] (Fig. 8; the newly prepared reconstituted enzyme complex has a slightly enlarged cycle time $\tau \approx 2$ s). A nonstructured synchronization curve was predicted from a model based on M (=8) states, but the actual measured synchronization curve is well structured. This discrepancy indicates that the enzymatic model used has to be modified.

In summary, the reaction model, based on a small number of chemical steps in the reaction cycle, failed to explain the value of the normalized memory time, the high percentage of

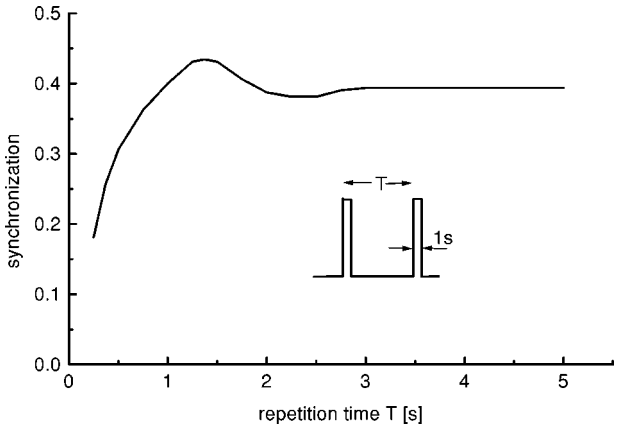

FIG. 7. The calculated synchronization of the enzymatic activity as a function of the repetition time of the light flashes is shown. A synchronization of one means that all enzymes work in phase, and a synchronization of zero means uncorrelated working enzymes. The total number of steps is kept constant ($M=8$). The last step in the reaction cycle was assumed to be light sensitive $f_8=500\ s^{-1}$ (with light) and $10\ s^{-1}$ (no light). For the other states ($i=1-7$), $b_i=1\ s^{-1}$, and $f_i=30\ s^{-1}$ were used.

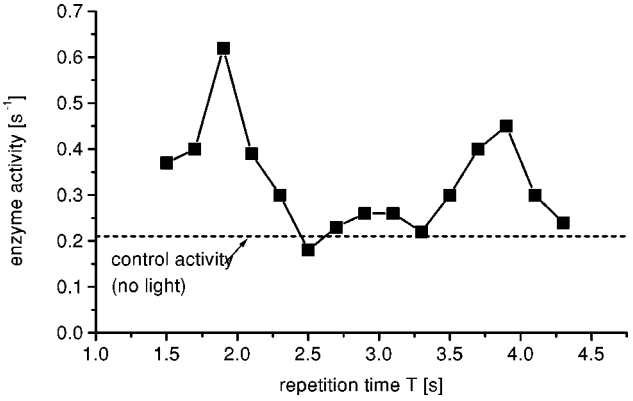

FIG. 8. The measured enzymatic activity of the reconstituted cytochrome P-450 complex is shown as a function of the repetition time of the light flashes [21].

synchronization, and the well-structured synchronization curve. Next, the influence of the number of states in the enzymatic reaction will be discussed.

CONFORMATIONAL SUBSTATES

First, the normalized memory time τ_M/τ of the enzymatic reaction is calculated for different number of states, M, in the cycle. τ_M/τ increases with increasing M. The calculated normalized memory time, τ_M/τ, is in accordance with the measured one (2.8 ± 0.5) for approximately 40–60 states.

Second, synchronization curves are calculated for different numbers of states in the cycle. The synchronization curve becomes well structured with a high percentage of synchronization for large numbers of states in the reaction cycle. A synchronization curve based on 40 states is shown in Fig. 9. The basic features of the experimentally determined curve are found: (i) The enzyme can be synchronized if the repetition time T_1 of the externally applied pulses is slightly smaller than the cycle time, τ. (ii) The enzyme can be synchronized at large repetition times, where the enzyme makes n free cycles between two proceeding externally applied pulses. The maximum of the synchronization is obtained for

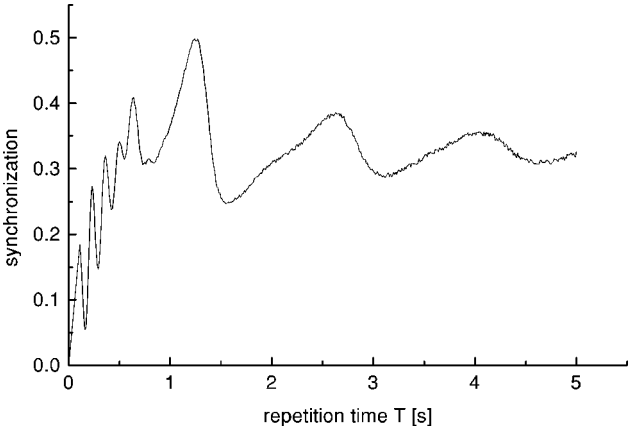

FIG. 9. The calculated synchronization of the enzymatic activity as a function of the repetition time of the light flashes is shown. The total number of steps is kept constant ($M=40$): $f_i=30\ \mathrm{s}^{-1}$ and $b_i=1\ \mathrm{s}^{-1}$ for $i=1-35$ and $f_i=500\ \mathrm{s}^{-1}$ (with light), $f_i=10\ \mathrm{s}^{-1}$, and $b_i=1\ \mathrm{s}^{-1}$ for $i=36-40$.

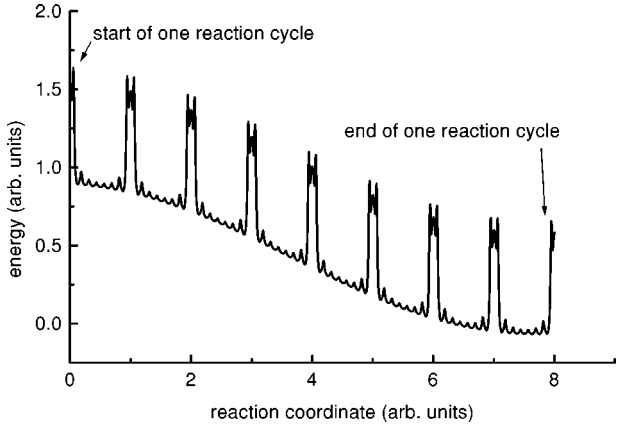

FIG. 10. A schematic representation of the landscape of an enzyme is shown.

repetition times which are the sum of T_1 and multiples of τ as $T_{n+1}=T_1+n\tau$. The calculated small sharp peaks at small repetition times are caused by several flashes in the time T_1. They are not yet observed in the experiment. The number of states in the reaction cycle can be estimated by comparing the calculated synchronization curve with the measured one. This rough estimation leads to 40–60 states in the reaction cycle.

In summary, the number of states in the reaction cycle is much higher than the number of distinct chemical states. The eight chemical states have to be replaced by approximately 40–60 physical states. Thus every chemical state contains approximately 5–7 distinct physical states.

What is the meaning of this huge number of states in the enzymatic reaction cycle? The concept of protein dynamics is used to understand the drastically increased number of states in the catalytic cycle. The protein dynamics of heme containing proteins was studied by several research groups using low-temperature flash photolysis [22]. Their results made it clear that the relaxation in the heme pocket is extremely complex, and the conformational substates of the proteins are important.

For small molecules such as O_2, the energetic state can be described by electronic, vibrational, and rotational terms. Proteins, however, are quite flexible, and have a very large number of degrees of freedom, which can accept many conformations. For them, a fourth term—the conformational energy—becomes important [22]. The energy hypersurface of a protein does not possess just one minimum like the small molecule O_2, but consists of a large number of valleys separated by possibly high ridges (Fig. 10). The energy landscape of a protein consequently is similar to that of other complex systems such as glasses and spin glasses. Evidence of the existence of the conformational states comes from, e.g., different types of observations: (i) the nonexponential time-dependence of protein processes, (ii) hole burning and inhomogeneous broadening of spectral lines, and (iii) large, inhomogeneous Debye–Waller factors.

A protein like P-450 can be regarded as a machine which is able to perform a special function. The enzymatic reaction of the cytochrome P-450 can be described by eight chemically distinguishable states as shown in Fig. 2. These are taxometric states, since each state can by characterized by a distinct chemical reaction. However, to understand the work-

ing machine every chemically distinguishable state of the protein has to be divided into several conformational substates. Thus, instead of having, e.g., eight rate equations, one deals with 40–60 rate equations. In the case of too many substates the discrete state variable can be replaced by a continuous one. Next, the enzymatic reaction will be described by using continuous states in the reaction cycle, and the relevant motion modes are derived.

ENZYME REACTION, BROWNIAN MOTION, AND FOKKER–PLANCK EQUATION

The state variable m, which characterizes a discrete physical state in the chemical reaction cycle, will now be replaced by a continuous state variable x. The following relation combines the continuous with the discrete variable

$$x = m\,\frac{2\pi}{M} = mK_M\,. \tag{3}$$

M is total number of states in the cycle. The propagation vector K_M $(=2\pi/M)$ describes the state change in the cycle. The transition probabilities f_i and b_i in the master equation (2) are regarded as x dependent. Every cycle starts when x is a multiple of 2π, and ends when x is increased by 2π. The forward and backward transition functions $f(x)$ and $b(x)$, as well as the continuous state probability $p(x)$, are periodic functions.

The master equation (2) of the enzymatic reaction is transformed into a Fokker-Planck equation if a Taylor series of $f(x)$ and $b(x)$ up to second order is used (see Appendix A),

$$\frac{\partial p}{\partial t} = \frac{\partial}{\partial x}\left\{ -F(x) + \frac{\partial}{\partial x}D(x)\right\} p(x). \tag{4}$$

The transition probabilities $f(x)$ and $b(x)$ describe the drift and the diffusion terms, $F(x)$ and $D(x)$, respectively.

$$F(x) = K_M[f(x) - b(x)], \tag{5}$$

$$D(x) = \frac{1}{2}K_M^2[f(x) + b(x)]. \tag{6}$$

The drift of the state probability, $p(x)$, through the reaction cycle is given by the first term on the right side of Eq. (4), and the diffusion of the state probability $p(x)$ by the second term. A physical approach of the enzymatic reaction is schematically shown in Fig. 11.

The kinetics of a chemical reaction can be considered in analogy to the motion of a particle in a double-well potential, as Kramers [9] and Brinkman [10] have shown. In the studies of Brownian motion of inert particles, one is principally concerned with the perpetual irregular motion exhibited by particles immersed in a fluid. The perpetual motion of the Brownian particle is maintained by the collisions with the molecules of the surrounding liquid [24]. The Brownian particle is kicked by a stochastic force, and it may leave the well and go either to the neighboring left or right well. In the high friction limit, where acceleration is neglected, the force balance equation per unit mass for the Brownian particle reads

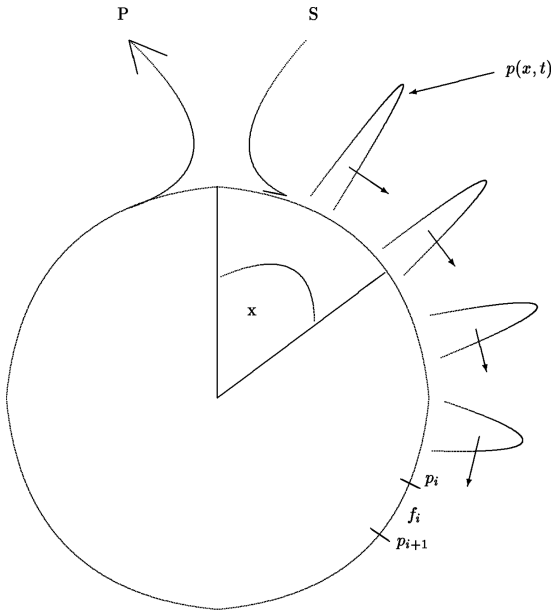

FIG. 11. Schematic representation of the enzymatic reaction.

$$\gamma\,\frac{dx}{dt} = -\,\frac{dV}{dx} + \Gamma(t), \tag{7}$$

with the friction coefficient γ, the potential $V(x)$, and the stochastic force $\Gamma(t)$. The position of the inert particle will vary stochastically because $\Gamma(t)$ is a stochastic quantity, and consequently x will become a stochastic quantity too. One, therefore, may ask for the probability to find the particle in the interval $(x, x+dx)$. Because x is a continuous variable we may ask for the probability density $P(x)$, also often called the probability distribution. The Langevin equation (7) can be transformed into a Fokker-Planck equation [24]

$$\frac{\partial P}{\partial t} = \frac{\partial}{\partial x}\left(-D^{(1)}(x) + \frac{\partial}{\partial x}D^{(2)}(x)\right) P(x,t) \tag{8}$$

The drift function $D^{(1)}(x)$ is obtained from the deterministic part of the Langevin equation, $D^{(1)} = -\gamma^{-1}\,dV/dx$. The diffusion function $D^{(2)}$ is obtained from the stochastic part of the Langevin equation. One obtains $D^{(2)} = \gamma^{-1}\,q/2$ in case of white noise [$\langle\Gamma(t)\rangle = 0$ and $\langle\Gamma(t)\Gamma(t')\rangle = q\,\delta(t-t')$, and q quantifies the noise strength].

The state of a chemical reaction can be considered in analogy to an inert particle in a potential well. The state variable x describes the position within the reaction cycle. The perpetual motion of the state variable is maintained by the thermal energy and the externally supplied energy. One can imagine that a fraction of the delivered energy is used, e.g., to create large fluctuating shape changes of the enzyme complex. Thus one expects a state-dependent stochastic force in the reaction cycle.

The Langevin equation, which describes the movement of a substrate molecule through the enzymatic reaction cycle, can be derived [24] from the corresponding Fokker-Planck equation (4),

$$\frac{dx}{dt} = h(x) + g(x)\Gamma(t). \tag{9}$$

As expected, the driving force $h(x)$, as well as the stochastic force $g(x)\Gamma(t)$, are state dependent. A white noise is assumed for $\Gamma(t)$ with a state-dependent strength $g(x)$. The driving force $h(x)$ is proportional to the difference of the forward and backward reactions. However, in addition, the x-dependent stochastic force creates a drift term, the so-called spurious drift or noise-induced drift [24]. It drives the system toward states where the diffusion is decreased.

$$h(x)=D^{(1)}(x)-\frac{1}{2}\frac{dD^{(2)}(x)}{dx}. \tag{10}$$

The stochastic force $g(x)$ is proportional to the square root of the diffusion term $D^{(2)}(x)$,

$$g(x)=D^{(2)}(x)^{1/2}. \tag{11}$$

The state-dependent stochastic force means that the quasitemperature is a function of the position of the reaction cycle.

A potential $V(x)$, which is relevant for the enzymatic reaction, can be derived from the driving force $h(x)$ [11],

$$h(x)=-\frac{dV(x)}{dx}. \tag{12}$$

As expected, this potential is proportional to the integral of the drift term, $D^{(1)}(x)$, but, in addition, a function of the state-dependent diffusion term, $D^{(2)}(x)$:

$$V(x)=-\int_0^x D^{(1)}(x)dx+\tfrac{1}{2}D^{(2)}(x). \tag{13}$$

The potential difference per cycle

$$\Delta V=-\int_0^{2\pi} D^{(1)}(x)dx \tag{14}$$

is simply given by the drift term, since the spurious drift plays only a role within the cycle. The potential difference has to be supplied from an external source in order to obtain the same physical state in every cycle [$V(x)=V(x+n2\pi)$].

In the case of constant forward and backward reaction coefficients, the potential is simply a straight line within one cycle,

$$V(x)=V(0)-D^{(1)}x=V(0)-K_M(f-b)x. \tag{15}$$

The potential function has a profile of a sawtooth if several cycles are regarded.

Our long term goal is to measure the steady-state distribution $p(x)$ within one reaction cycle for synchronized enzymes. Then the experimental results are compared with theoretical predictions [Eq. (4)], where the state-dependent drift, $D^{(1)}(x)$, and diffusion, $D^{(2)}(x)$, terms, or the state-dependent forward, $f(x)$, and backward, $b(x)$, reaction coefficients are fitting functions. We hope to find the predicted state dependence in the driving force as well as in the stochastic force. Next, the Fokker-Planck equation will be solved for a special case where the forward and backward reaction functions are constants.

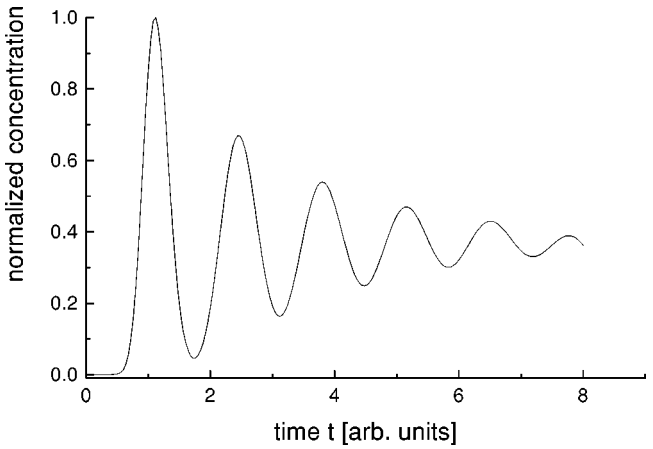

FIG. 12. The normalized occupation of the last step is calculated by means of the Fokker-Planck equations and shown as a function of time. At $t=0$ the reaction is switched on.

Constant transition coefficients

The Fokker-Planck equation is a parabolic differential equation if the transition probabilities f and b are constant,

$$\frac{\partial p}{\partial t}=-F\frac{\partial p}{\partial x}+D\frac{\partial^2 p}{\partial x^2}. \tag{16}$$

This partial differential equation can be solved by making a separation ansatz

$$p(x,t)=e^{\lambda t}\Theta(x). \tag{17}$$

The eigenvalues λ are obtained by inserting Eq. (17) into Eq. (16),

$$\lambda_k=-ikF-k^2D. \tag{18}$$

The solution then reads

$$p(x,t)=\sum_{k=-\infty}^{\infty}(C_k e^{i[kx-\omega_k t)]})e^{-k^2Dt}, \tag{19}$$

where the eigenfunction $\Theta(x)$ is approximated by a Fourier series

$$\Theta(x)=\sum_{k=-\infty}^{\infty}C_k e^{ikx}. \tag{20}$$

The complex numbers C_k are given by the starting conditions. Solution (19) has the structure of a damped traveling wave (see Fig. 12). The drift term F determines the frequency ω_k of the traveling wave,

$$\omega_k=-k\,F=-kK_M(f-b). \tag{21}$$

As expected, the wave is running clockwise for $f>b$ and counterclockwise for $f<b$. No traveling wave is expected for zero drift.

The predictions of this simple model can be compared with already performed experiment: (i) The transduction coefficient, k_E, can be measured and, thus, the drift term F can

be determined as $F=2\pi k_E$. (ii) The diffusion term D determines the damping time τ_M of the traveling wave

$$\tau_M=\frac{1}{k^2D}=\frac{2}{k^2K_M^2(f+b)}. \tag{22}$$

This damping time τ_M is identical with the previously discussed memory time of the enzymatic reaction. τ_M can be measured and, thus, the diffusion term D can be determined as $D=1/\tau_M$ for the $k=1$ mode. The ratio of drift and diffusion coefficient is simply the normalized memory time multiplied by 2π:

$$\frac{F}{D}=2\pi\frac{\tau_M}{\tau}. \tag{23}$$

In the Michaelis-Menten approximation, the enzymatic reaction is characterized by one coefficient—the transduction coefficient k_E, which is proportional to the drift coefficient of the Fokker-Planck equation. The drift coefficient $F(=2\pi k_E)$ characterizes the deterministic part of the enzymatic reaction. The diffusion coefficient $D(=1/\tau_M)$ of the Fokker-Planck equation is a second coefficient which characterizes the stochastic part of the enzymatic reaction.

Next the forward and backward coefficients will be determined. In the approximation used, one has three unknown coefficients f, b, and K_M, which can be determined by the experimentally determined cycle time τ, the memory time τ_M, and the number of states, M. The forward transition coefficient f and the ratio of backward and forward coefficient, b/f, are

$$f=\frac{M}{2\pi}\frac{1}{\tau}+\frac{1}{2\pi}\left(\frac{M}{2\pi}\right)^2\frac{1}{\tau_M}, \tag{24}$$

$$\frac{b}{f}=\frac{1-\dfrac{2\pi^2}{M}\dfrac{\tau_M}{\tau}}{1+\dfrac{2\pi^2}{M}\dfrac{\tau_M}{\tau}}. \tag{25}$$

One obtains $f=6.5\ \mathrm{s}^{-1}$ and $b\approx 0.2\ \mathrm{s}^{-1}$, with $\tau=1.54$ s, $\tau_M/\tau=2.8$, and $M\approx 60$. As expected for a good working chemical production plant, the back reaction coefficient is very small compared with the forward reaction. Next, the Fokker-Planck equation will be solved for a state-dependent forward reaction.

State-dependent forward reaction

An enzymatic reaction with its characteristic reaction cycle cannot simply be explained by constant drift and diffusion coefficient, since rate-limiting chemical reaction steps are known. Let us assume a scenario with a fast state-dependent forward reaction $f(x)$, but a slow backward reaction $b\ll f$, as, e.g., $f(x)\neq 0$ and $b=0$. The state-dependent forward reaction function can be described by a Fourier series

$$f(x)=f_0\sum_k F_k e^{ikx}, \tag{26}$$

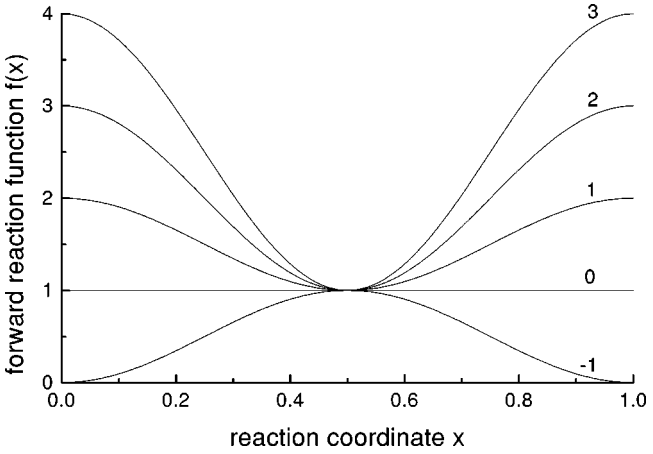

FIG. 13. The forward reaction function $f(x)$ for various values of $\hat{v}$.

where f_0 determines the strength of the reactions, and F_k the profile within the reaction cycle. f_0 as well as F_k should be determined by experiments. We do not have such detailed and precise experiments. To proceed further, a simple sinusoidal reaction profile, as seen in Fig. 13, is assumed: $v(x)=\hat{v}\cos^2(x/2)$. The amplitude of the state-dependent forward reaction function is described by $\hat{v}$.

The Fokker-Planck equation (4) can be written in dimensionless units if a dimensionless time $t'=f_0K_Mt$ is introduced:

$$f_0\frac{\partial p}{\partial t'}=-\frac{\partial}{\partial x}\{f(x)p(x,t')\}+\frac{K_M}{2}\frac{\partial^2}{\partial x^2}\{f(x)p(x,t')\}. \tag{27}$$

Again, the separation ansatz (17) can be used to determine the eigenvalues, since the periodic function is only state but not time dependent. The unknown eigenfunction $\Theta(x)$ is approximated by a Fourier series (20).

The eigenvalues λ_k are obtained by inserting Eqs. (17) and (20) into Eq. (27),

$$\lambda_kC_k=-(ik+\tfrac{1}{2}K_Mk^2)\{\tfrac{1}{4}\hat{v}C_{k-1}+(1+\tfrac{1}{2}\hat{v})C_k+\tfrac{1}{4}\hat{v}C_{k+1}\}. \tag{28}$$

One obtains $\lambda_0C_0=0$ for $k=0$. The eigenvalue λ_0 is zero, since the total number of enzymes involved $(2\pi C_0=\int p(x)dx\neq 0)$ is described by the coefficient C_0. The other eigenvalues λ_k can be calculated in the following way: Two tridiagonal systems of equations, are obtained by treating separately the symmetric and antisymmetric eigenfunctions Θ_s, and Θ_a, and splitting the eigenvalue λ into its real and imaginary parts $(\lambda_k=\mu_k+i\omega_k)$

$$\tfrac{1}{4}\hat{v}C_{k-1}+\left(1+\frac{\mu}{K_Mk^2}+\frac{1}{2}\hat{v}\right)C_k+\tfrac{1}{4}\hat{v}C_{k+1}=0, \tag{29}$$

$$\tfrac{1}{4}\hat{v}C_{k-1}+\left(1+\frac{\omega}{k}+\frac{1}{2}\hat{v}\right)C_k+\tfrac{1}{4}\hat{v}C_{k+1}=0. \tag{30}$$

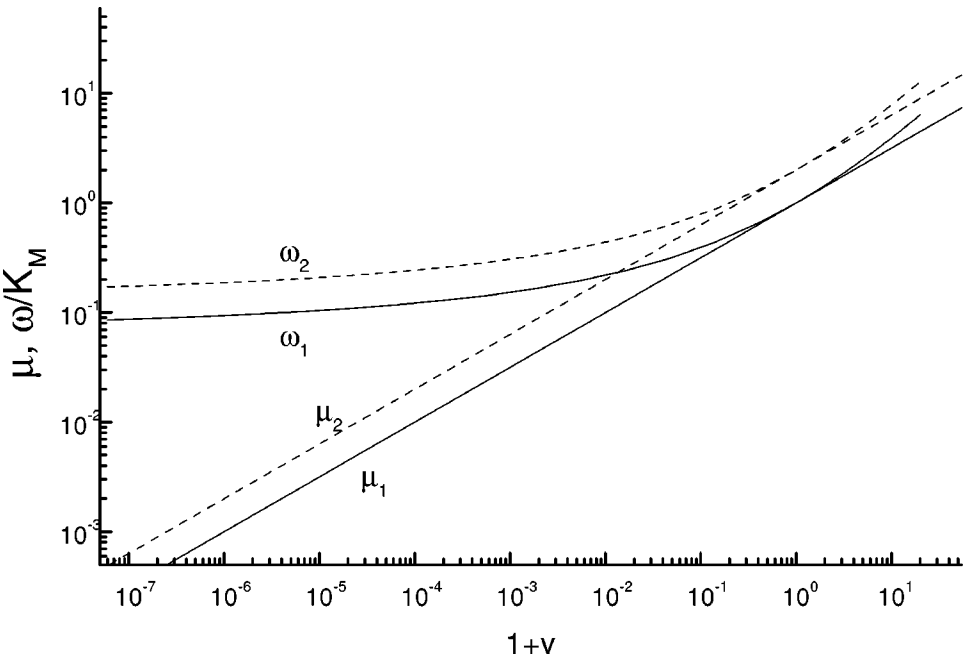

FIG. 14. Normalized real (μ) and imaginary (ω) part of the first two eigenvalues of the cosine potential are shown.

The solution for the eigenvalues is obtained by solving these tridiagonal equation system by the continued fraction technique [24]. The first and second eigenvalue, are shown as a function of $1+\hat{v}$ in Fig. 14.

The imaginary part ω of the eigenvalue describes the frequency of the traveling wave in the chemical reaction cycle. First, the frequency $\omega_1(\hat{v})'$ is calculated from Eq. (21) by taking the mean of the forward reaction function $\omega_1(\hat{v})'=\omega_1(0)(1+\hat{v})$. In the case of no state-dependent function, the frequency $\omega_1(0)$ is $K_M f_0$. In this approximation, the frequency increases linearly with the amplitude $\hat{v}$ of the state-dependent forward reaction function. However, the frequency $\omega(\hat{v})$ calculated from the state-dependent forward reaction function [Eq. (30)] can be described by a power law

$$\omega_k(\hat{v})=k\omega_1(0)(1+\hat{v})^{\nu}. \tag{31}$$

The exponent ν, is determined from Fig. 14 to be 0.50. The discrepancy between the exact calculation and the approximation is easy to understand, since the low values of the forward reaction function are more strongly weighted than the high values: The traveling wave moves faster as expected from the mean forward reaction approximation if $\hat{v}<0$, and slower if $\hat{v}>0$. The wave stops traveling if the forward reaction is zero at a certain position in the reaction ($\hat{v}\rightarrow -1$), and thereby the eigenvalue ω approaches 0.

The real part μ of the eigenvalue describes the damping of the traveling wave in the chemical reaction cycle. First, the damping coefficient, $\mu_1(\hat{v})'$, is calculated from Eq. (21) by taking the mean forward reaction function $\mu_1(\hat{v})'=\mu_1(0)(1+\hat{v})$. In the case of no state-dependent function, the damping coefficient $\mu_1(0)$ is $K_M^2 f_0/2$. In this approximation, the damping coefficient increases linearly with the amplitude of the state-dependent forward reaction function. However, the damping coefficient $\mu_1(\hat{v})$, calculated from the state-dependent forward reaction function [Eq. (22)], can be characterized by two features: (i) The damping reaches a finite value for $\hat{v}\rightarrow -1$. Here, one has to remember that in this case the frequency of the traveling wave approaches zero. (ii) A power law is obtained for $\hat{v}>0$,

$$\mu_k=k^2\mu_1(0)(1+\hat{v})^{\eta}. \tag{32}$$

The exponent $\eta=0.66$ is determined from Fig. 14.

This calculation shows that the enzymatic reaction cannot simply be approximated by taking the average of the forward reaction function. To proceed further, one needs new types of experiments where the substrate molecule is observed during the enzymatic reaction. Next, the Fokker-Planck equation will be solved for a state- and time-dependent forward reaction function $f(x,t)$.

State- and time-dependent forward reaction

An enzymatic reaction can be influenced by an external signal S_{ex}. For example, light can alter the enzymatic reactivity if one of the active groups of the enzyme complex absorbs light. We showed experimentally that the enzyme activity can be enhanced by light [17] and that the catalytic cycle of the enzymes can be synchronized by periodically applied light flashes [18]. Let us assume again a scenario with a fast forward reaction $f(x,S_{\mathrm{ex}})$, but a negligible backward reaction $b\approx 0$. In addition, the forward reaction should be a function of an extracellular signal. The forward reaction function can be described by a Fourier series

$$f(x)=f_0\sum_k F_k(S_{\mathrm{ex}})e^{ikx}. \tag{33}$$

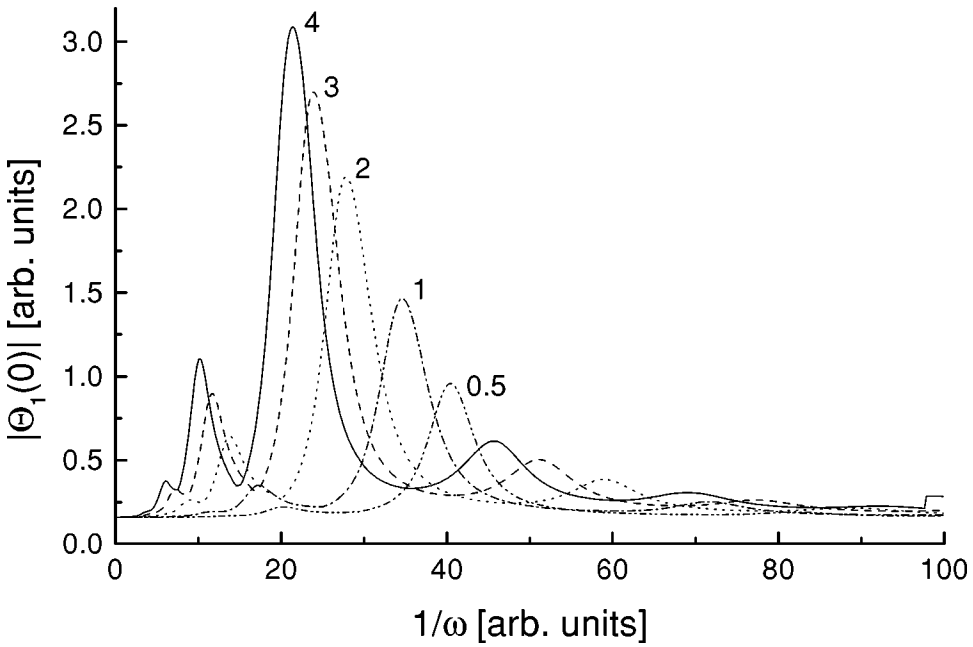

FIG. 15. The typical resonance behavior shown for the first eigenfunction $\Theta_1(x=0)$. Five curves with different values of $\hat{v}$ are plotted against the inverse of the frequency ω.

The strength of the enzymatic reaction and its profile are f_0 and $F_k(S_{ex})$, respectively, which should be determined by experiments, but we do not have such detailed and precise experiments. To proceed further, a simple sinusoidal reaction profile is assumed: $f(x)=1+\hat{v}(t)\cos^2(x/2)$. The amplitude $\hat{v}(t)=\hat{v}_0\sin\omega' t$ of the state-dependent forward reaction coefficient is temporal modulated with the external frequency ω'.

Note that the drift term $h(x,t)$ in the Langevin equation (9), as well as the potential $V(x,t)$, are time dependent. Thus one has a parametric process, and expects that the response is maximum when the externally applied frequency is approximately equal to the internal frequency (parametric resonance). Additionally, one deals with a system where stochastic processes are involved. Stochastic resonance is an effect which is manifested in multistable nonlinear systems driven simultaneously by noise and a weak periodic function. These stochastic processes can help to change the enzymatic state, and the enzymatic activity can be enhanced if the frequency of the externally applied signal is approximately equal to the intrinsic frequency (stochastic resonance).

The solution of the Fokker-Planck equation with a periodic state- and time-dependent coefficients can be constructed by using Floquet's theorem

$$p(x,t)=e^{\mu t}\sum_n d_n e^{in\omega t}\Theta_n(x). \tag{34}$$

The unknown eigenfunction $\Theta_n(x)$ can again be expressed by a Fourier series. The general solution then reads

$$p(x,t)=e^{\mu t}\sum_n d_n\sum_k c_n^k\, e^{in\omega t}e^{ikx}. \tag{35}$$

The coefficients d_n and c_n^k are given by the starting conditions.

The eigenvalue, $\lambda_k(=\mu_k+i\omega_k)$, is obtained by inserting Eqs. (33)–(35) into Eq. (27),

$$\begin{aligned}(\mu_k+in\omega_k)c_n^k=&-\left(ik+\frac{K_M}{2}k^2\right)\{\tfrac{1}{4}\hat{v}_0c_{n-1}^{k-1}+(1+\tfrac{1}{2}\hat{v}_0)c_{n-1}^k\\&+\tfrac{1}{4}\hat{v}_0c_{n-1}^{k+1}-\tfrac{1}{8}(\hat{v}_0c_n^{k-1}+\hat{v}_0c_n^{k+1}\\&+\hat{v}_0c_{n+1}^{k-1}+\hat{v}_0c_{n+1}^{k+1})\}.\end{aligned} \tag{36}$$

One obtains $\mu_0c_0^0=0$ for $k=0$ and $n=0$. The real eigenvalue μ_0 is zero, since c_0 is a positive quantity which describes the total number of enzymes.

The discussion below will be restricted to the simple case with $\mu_0=0$, where the probability density $p(x,t)$ is then described by a sum of *undamped* traveling waves,

$$p(x,t)=\sum_n d_n\sum_k c_n^k e^{i(n\omega t+kx)}$$

$$=\sum_n d_n e^{in\omega t}\Theta_n(x).$$

Only the first eigenfunction $\Theta_1(x)$ is calculated to show the basic features of how an enzyme can be enslaved by an external signal. Because $p(x,t)$ must be real, $\Theta_{-1}(x)$ is given by the complex conjugate of $\Theta_1(x)$.

Let us now look how $\Theta_1(x)$ depends on the frequency ω. For this purpose we determine the quantities c_1^k in dependence of ω and vary the height of the potential $\hat{v}$. The results are given in Fig. 15, where $|\Theta_1(0)|$ is plotted against $1/\omega$. The calculated curve demonstrates that the amplitude of the undamped waves is a function of the external frequency. The effect is maximum if the external frequency is approximately the same as the intrinsic frequency. The calculated maximum

is very sharp, as actually observed by the experiments (see Fig. 3 of Ref. [18]). An enzymatic reaction can be enslaved by an external signal, and the model of the parametric and stochastic resonance fits the experimental data very well.

SUMMARY

The catalytic cycle of an enzyme is quite well approximated by a set of differential equations, first order in time, if the number of differential equations is much higher than the number of rate-limiting states. Every chemically well-defined taxometric state again has several physically well-distinguished states (conformational states) which are important for the working enzyme.

A system having many discrete states can be approximated by a system having continuous states. The system is now characterized by a probability density function that satisfies a second-order partial differential equation. The drift term is responsible for the mean duration of the catalytic reaction and the diffusion term for the width of the cycle time distribution, or in other words, the drift term is the cause for a traveling probability wave within the reaction cycle and the diffusion term is the cause for the damping of the traveling wave.

An enzymatic reaction can be enslaved by an external signal if the damping time is much longer than the cycle time. In addition, at least one of the rate-limiting steps in the reaction cycle has to be sensitive to the external signal.

ACKNOWLEDGMENTS

We are grateful to Professor Dieter Müller-Enoch for his support and encouragement. This work was supported in part by ''Fonds der chemischen Industrie'' and ''Fondation de France.'' One of us (M.S.) acknowledges financial support from the ''Deutsche Forschungsgemeinschaft.'' One of us (H.G.) is grateful to the ''Fondation de France'' for giving him the opportunity to work in Paris.

APPENDIX A: FOKKER-PLANCK EQUATION

$$\dot{p}_1 = -(f_1 + b_1)p_1 + f_M p_M + b_2 p_2,$$

$$\dot{p}_m = -(f_m + b_m)p_m + f_{m-1}p_{m-1} + b_{m+1}p_{m+1},$$

$$m = 2, \ldots, M-1,$$

$$\dot{p}_M = -(f_M + b_M)p_M + f_{M-1}p_{M-1} + b_1 p_1.$$

After introducing a new variable x,

$$x = 2\pi \frac{m}{M} = mK_M,$$

we obtain

$$\dot{p}(x) = f(x-K_M)p(x-K_M) - f(x)p(x) + b(x+K_M) \times p(x+K_M) - b(x)p(x).$$

Taylor expansion of the probabilities is the main step to achieve a partial differential equation of the diffusion type.

$$p(x-K_M) = p(x) - K_M \frac{\partial p}{\partial x} + \frac{1}{2}K_M^2 \frac{\partial^2 p}{\partial x^2} \cdots,$$

$$p(x+K_M) = p(x) + K_M \frac{\partial p}{\partial x} + \frac{1}{2}K_M^2 \frac{\partial^2 p}{\partial x^2} \cdots.$$

If we stop the expansion after the order K_M^2, we obtain the following equation:

$$\frac{\partial p}{\partial t} = \frac{\partial}{\partial x}\left\{ -K_M[f(x) - b(x)] + \tfrac{1}{2}K_M^2 \frac{\partial}{\partial x}[f(x) + b(x)] \right\} p(x). \tag{A1}$$

APPENDIX B: TRIDIAGONAL RECURRENCE RELATION

Using matrix notation, Eq. (36) can be written as

$$\mathbf{A}_1 \vec{\mathbf{c}}_{n-1} + (\mathbf{A}_0 - in\omega\mathbf{E})\vec{\mathbf{c}}_n + \mathbf{A}_1 \vec{\mathbf{c}}_{n+1} = 0. \tag{B1}$$

This tridiagonal vector recurrence relation again can be solved by means of continued fractions if we truncate this system at an upper limit $n = N$. The vector recurrence relation can be solved if we define new matrices $\mathbf{S}_n$ in the following way:

$$\vec{\mathbf{c}}_{n+1} = \mathbf{S}_n \cdot \vec{\mathbf{c}}_n. \tag{B2}$$

Inserting this in Eq. (B1), we obtain recurrence relations between $\mathbf{S}_n$,

$$\mathbf{S}_{n-1} = -\{(\mathbf{A}_0 - in\omega\mathbf{E}) + \mathbf{A}_1\mathbf{S}_n\}^{-1}\mathbf{A}_1, \tag{B3}$$

Using matrix inversion routines we can solve Eq. (B3) numerically up to $n = 1$. At this stage the vector $\vec{\mathbf{c}}_1$ and therefore all other vectors $\vec{\mathbf{c}}_n$ can be determined, because $\vec{\mathbf{c}}_0$ is known:

$$\vec{\mathbf{c}}_1 = \mathbf{S}_0 \cdot \vec{\mathbf{c}}_0, \tag{B4}$$

$$\vec{\mathbf{c}}_n = \mathbf{S}_n \cdot \mathbf{S}_{n-1} \ldots \mathbf{S}_1 \cdot \mathbf{S}_0 \cdot \vec{\mathbf{c}}_0. \tag{B5}$$

[1] I. H. Segel, *Biochemical Calculations* (Wiley, New York, 1976).

[2] N. S. Goel and N. Richter-Dyn, *Stochastic Models in Biology* (Academic, New York, 1974).

[3] N. G. van Kampen, *Stochastic Processes in Physics and Chemistry* (North-Holland, Amsterdam, 1981).

[4] N. Wax, *Noise and Stochastic Processes* (Dover, New York, 1954).

[5] W. Schottky, Ann. Phys. (Leipzig) **68**, 157 (1922).
[6] H. Nyquist, Phys. Rev. **32**, 110 (1928).
[7] M. Lax, Rev. Mod. Phys. **32**, 25 (1960).
[8] M. Schienbein, K. Franke, and H. Gruler, Phys. Rev. E **49**, 5462 (1994).
[9] H. A. Kramers, Physica (Amsterdam) **7**, 284 (1940).
[10] H. C. Brinkmann, Physica (Amsterdam) **22**, 149 (1956).
[11] H. Haken, *Synergetics* (Springer-Verlag, Berlin, 1983).
[12] *Cytochrome P-450*, edited by P. R. Ortiz de Montellano (Plenum, New York, 1986).
[13] F. P. Guengerich, G. A. Dannan, S. T. Wright, M. V. Martin, and L. S. Kaminsky, Biochemistry **21**, 6019 (1982).
[14] D. Müller-Enoch, P. Churchill, S. Fleischer, and F. P. Guengerich, J. Biol. Chem. **259**, 8174 (1984).
[15] F. P. Guegenerich, Prog. Drug Metabolism **10**, 1 (1987).
[16] D. W. Nebert, and F. J. Gonzalez, Annu. Rev. Biochem. **59**, 945 (1987).
[17] W. Häberle, H. Gruler, Ph. Dutkowski, and D. Müller-Enoch, Z. Naturforsch. C **45**, 273 (1990).
[18] H. Gruler and D. Müller-Enoch, Eur. Biophys. J. **19**, 217 (1991).
[19] B. Hess and A. Mikhailov, Biophys. Chem. **58**, 365 (1994).
[20] P. E. White and M. J. Coon, Annu. Rev. Biochem. **49**, 315 (1980).
[21] S. Kiener, Diplomarbeit, Universität Ulm, 1994.
[22] H. Frauenfelder *et al.*, Annu. Rev. Biophys. Biophys. Chem. **17**, 451 (1988).
[23] A. L. Lehninger, *Biochemistry* (Worth, New York, 1975).
[24] H. Risken, *Fokker-Planck Equation* (Springer-Verlag, Heidelberg, 1984).